CHEMICAL ENGINEERING TRANSACTIONS
VOL. 70, 2018
A publication of AIDIC
The Italian Association of Chemical Engineering
Online at www.aidic.it/cet
Guest Editors: Timothy G. Walmsley, Petar S. Varbanov, Rongxin Su, Jiří J. Klemeš

ISBN 978-88-95608-67-9; **ISSN** 2283-9216
DOI: 10.3303/CET1870140

Efficient Optimization of Recuperator Design for Aero Engine Applications

Kostas Germakopoulos[a], Christina Salpingidou[b], Zinon Vlahostergios[c,*], Dimitrios Misirlis[d], Michael Flouros[e], Fabian Donus[e], Athanasios I. Papadopoulos[f], Panos Seferlis[a], Kyros Yakinthos[b]

[a]Aristotle University of Thessaloniki, Machine Dynamics Laboratory, Egnatia Street, 54124, Thessaloniki, Greece
[b]Aristotle University of Thessaloniki, Laboratory of Fluid Mechanics and Turbomachinery, Egnatia Street, 54124, Thessaloniki, Greece
[c]Democritus University of Thrace, Department of Production and Management Engineering, Laboratory of Fluid Mechanics and Hydrodynamic Machines, Xanthi, 67100, Greece
[d]Technological Educational Institute of Central Macedonia, Department of Mechanical Engineering TE, Terma Magnesias 62124 Serres, Greece
[e]MTU Aero Engines AG, Dachauer Strasse 665, Munich, Germany
[f]Centre of Research and Technology-Hellas, 6th klm. Harilaou-Thermis Rd, 57001, Thermi Thessaloniki, Greece
zinonv@eng.auth.gr

This work is focused on the optimization of the geometrical characteristics of a recuperator developed for aero engine applications, taking into consideration the aero engine geometrical constraints and limitations, in order to achieve feasible and implementable recuperator designs. For this reason, dedicated numerical surrogate tools were developed through which the effect of major geometrical features such as recuperator diameter, length, tubes arrangement and alignment could be directly included in order to assess their effect to recuperator operational performance characteristics such as recuperator effectiveness and inner/outer pressure losses. A large part of these activities was focused on the development of a nonlinear surrogate model incorporating the major geometrical features of the recuperator. In this tool, high-fidelity correlations regarding pressure losses and heat transfer, derived through experimental measurements and detailed CFD computations, were incorporated. Based on this model the recuperator performance was optimized using the simulated annealing algorithm resulting in the identification of recuperator design which can combine operational superiority with feasibility and implementation potential.

1. Introduction

The last decades, the European Advisory Council for Aviation Research and Innovation in Europe (ACARE, 2012) has set a Strategic Research Agenda (SRIA) towards the reduction of pollutant emissions in a sustainable way, targeting a reduction of 75 % for CO_2 and 90 % for NOx emissions by the year 2050. In order to fulfill these targets, many technologies have been developed and are under research by collaborations of European aero engine industries and Universities. A large number of research activities have been focused on the development of waste heat energy systems in order to exploit the high thermal content of aero engine exhaust gas and reduce fuel consumption and pollutant emissions. These systems are based on the integration of advanced design recuperators inside the aero engine hot-gas exhaust nozzle in order to preheat the compressor discharge air before the latter enters the combustion chamber. As a result, less fuel is required for the aero engine operation resulting in significant specific fuel consumption reduction with direct environmental and economic benefits. For the maximization of the benefits of recuperators installation, a compromise between the exploited waste heat in relation to the imposed pressure losses must be taken into consideration in order to achieve an overall advantage in the aero engine thermodynamic cycle performance. Furthermore, during the design stages of the recuperators, it is of prime importance to take into account the effect of the recuperator weight in order to achieve

Please cite this article as: Germakopoulos K., Salpingidou C., Vlahostergios Z., Misirlis D., Flouros M., Donus F., Papadopoulos A.I., Seferlis P., Yakinthos K., 2018, Efficient optimization of recuperator design for aero engine applications , Chemical Engineering Transactions, 70, 835-840 DOI:10.3303/CET1870140

a reliable and realistic quantification of the recuperator impact on aero engine performance, through the incorporation of installation effects.

This work is focused on the optimization of the geometrical characteristics of a recuperator developed for aero engine applications, taking into consideration the aero engine geometrical constraints and limitations, in order to achieve feasible and implementable recuperator designs. The analysis was based on the tubular heat exchanger recuperator of elliptical profiles which was developed and invented by MTU Aero Engines AG, presented in Figure 1a, while the thermodynamic conditions for the recuperator performance assessment were derived from the Intercooled Recuperated Aero (IRA) engine concept cycle, Figure 1b, combining both intercooling and recuperation. The IRA engine concept has been investigated in various European research projects such as the NEW Aero engine Core concepts – (NEWAC) and the Low Emissions Core-Engine Technologies – (LEMCOTEC) projects.

At the present work, targeting the optimization of the recuperator design, dedicated numerical surrogate tools were developed through which the effect of major geometrical features such as recuperator diameter, length, tubes arrangement and alignment could be directly included in order to assess their effect to recuperator operational performance characteristics such as recuperator effectiveness and inner/outer pressure losses. A large part of these activities was focused on the development of a nonlinear surrogate model incorporating the major geometrical features of the recuperator. In this tool high-fidelity correlations regarding pressure losses and heat transfer, derived through experimental measurements and detailed CFD computations (Salpingidou et al., 2016), were incorporated. Based on this model the recuperator performance was optimized using the simulated annealing (SA) algorithm resulting in the identification of recuperator design which can combine operational superiority with feasibility and implementation potential.

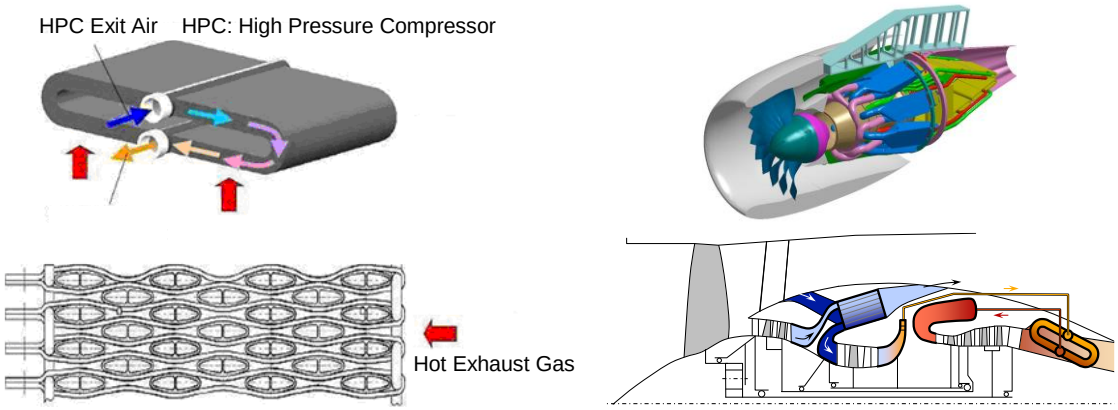

Figure 1: (a) The heat exchanger developed by MTU Aero Engines AG; (b) Intercooled Recuperative Aero-engine Concept.

2. Recuperator core performance characteristics

The recuperator effect on the aero engine performance is described by the recuperator thermal effectiveness and the induced pressure losses for both flow streams (inner flow-cold air and outer flow-hot-gas). The overall recuperator impact on the aero engine cycle is defined by the trade-off between the positively contributing achieved heat transfer rate and the detrimental effect of the imposed inner and outer pressure losses.

The inlet/outlet temperatures of the hot-gas and the cold air are denoted by $T_h \in \mathbb{R}^2$ and $T_c \in \mathbb{R}^2$, respectively. That is, $T_h(1), T_c(1)$ are the inlet temperatures and $T_h(2), T_c(2)$ are the outlet temperatures. Similarly, the inlet/outlet pressures of the hot-gas and the cold air are denoted by $P_h \in \mathbb{R}^2$ and $P_c \in \mathbb{R}^2$, respectively. The inlet conditions $T_h(1), T_c(1), P_h(1), P_c(1)$ and the mass flow rates $\dot{m}_h, \dot{m}_c$ of the outer and inner flow, respectively, were considered constant and equal to the corresponding properties of the IRA engine for average cruise conditions.

The thermodynamic properties of the fluids were calculated using the Peng-Robinson equation of state (Pratt, 2001). In particular, the Peng-Robinson equation, defines the air density ρ as a function of temperature and pressure and the air heat capacity C_p as a function of temperature. That is, $\rho(T, P)$ and $C_p(T)$ are the air density and heat capacity, respectively, at temperature T and pressure P. Using Sutherland's law (Anderson, 2011), the dynamic viscosity of air μ is expressed as a function of temperature. That is, $\mu(T)$ denotes the dynamic viscosity of air at temperature T. The kinematic viscosity of air ν can be written as $\nu = \mu/\rho$.

The mean velocity of the outer flow u_h is defined by the equality $u_h(T,P,\theta,r,R) = \dot{m}_h/\big(\rho(T,P)A_h(\theta,r,R)\big)$, where $A_h(\theta,r,R) = \pi L_H(\theta,r,R)(r+R)$ is the outer flow mean frontal area and $L_H(\theta,r,R) = (R-r)/\sin\theta$ is the heat exchanger (HEX) length (Figure 2). The mean velocity of the inner flow u_c is defined by Eq(1)

$$u_c(T,P,g,\theta,r,R,N_T,N_F) = \dot{m}_c/\big(\rho(T,P)A_c(g,\theta,r,R,N_T,N_F)\big), \tag{1}$$

where $A_c(g,\theta,r,R,N_T,N_F) = \big(N_f L_H(\theta,r,R)/g\big)N_T A$ is the total tubes feed area, g is the normal distance between the elliptic tubes of the same column, N_T is the number of tubes in an outer flow path, N_f is the number of feed collectors and A is the elliptic tube cross section area. Now, the Reynolds numbers Re_h and Re_c (based on the tube hydraulic diameter d) for the outer and inner flow, respectively, can be written as $Re_h = u_h d/v$ and $Re_c = u_c d/v$.

For the accurate calculation of the recuperator effectiveness, outer and inner pressure losses dedicated correlations were used. These correlations were extracted through detailed CFD computations and experimental measurements. More details are provided in Yakinthos et al. (2015).

For $x \in \mathbb{R}^2$ the symbol $\overline{x}$ denotes the number $\big(x(1)+x(2)\big)/2$. Let g,θ,r,R,N_T and N_F be fixed, and let $\overline{\rho}_h = \rho\big(\overline{T}_h,\overline{P}_h\big), \overline{\mu}_h = \mu\big(\overline{T}_h\big), \overline{\nu}_h = \nu\big(\overline{T}_h,\overline{P}_h\big)$ and $\overline{u}_h = u_h\big(\overline{T}_h,\overline{P}_h,\theta,r,R\big)$. Then, the outer flow stream pressure loss, corresponding to the pressure loss of the hot-gas flow passing around the elliptic tubes, is given by Eq(2)

$$P_h(1) - P_h(2) = \Big((a_0 + a_1\overline{\nu}_h)\overline{\mu}_h + \overline{\rho}_h\big(b_0 + b_1\overline{\nu}_h + b_2\overline{\nu}_h^2\big)\overline{u}_h\Big)\overline{u}_h L(N_T)/L_R. \tag{2}$$

The viscous pressure loss coefficients a_i and the inertial pressure loss coefficients b_i, are constant and were calibrated as described in Yakinthos et al. (2015). The constant L_R is the reference length used for the calibration of the pressure loss coefficients and $L(N_T)$ is the heat exchanger thickness.

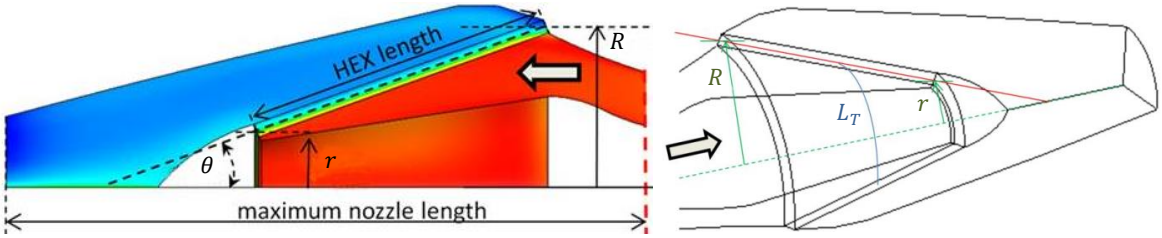

Figure 2: Geometrical parameters for recuperators following the CORN concept (Misirlis et al., 2017).

Let $\overline{\rho}_c = \rho\big(\overline{T}_c,\overline{P}_c\big), \overline{u}_c = u_c\big(\overline{T}_c,\overline{P}_c,g,\theta,r,R,N_T,N_F\big), \overline{Re}_c = Re_c\big(\overline{T}_c,\overline{P}_c,g,\theta,r,R,N_T,N_F\big)$. Then, the inner flow (cold air) pressure loss, is given by Eq(3)

$$P_c(1) - P_c(2) = 0.5\overline{f}_c(L_T(r,R,N_F)/d)\overline{\rho}_c\overline{u}_c^2, \quad \overline{f}_c = c_1\big(\ln\overline{Re}_c\big)^{c_2} \tag{3}$$

where $\overline{f}_c$ corresponds to the inner flow friction coefficient and $L_T(r,R,N_F) = \pi(r+R)/N_F$ is the mean tubes length (Figure 2). This approach is very similar to the Moody chart approach found in literature, with the difference that dedicated pressure loss coefficients (c_1, c_2) were used, which were calibrated after detailed CFD calculations.

Let $Pr(T)$ be the Prandtl number at temperature T, that is $Pr(T) = C_p(T)\mu(T)/k(T)$, where $k(T)$ is the air thermal conductivity (at temperature T), and let $\overline{Re}_h = Re_h\big(\overline{T}_h,\overline{P}_h,\theta,r,R\big)$, $\overline{Pr}_h = Pr\big(\overline{T}_h\big)$ and $\overline{Pr}_c = Pr(\overline{T}_c)$. The calculation of the thermal effectiveness of the recuperator was based on the calculation of the heat transfer coefficients $\overline{h}_h = k(\overline{T}_h)\overline{Nu}_h/d$ and $\overline{h}_c = k(\overline{T}_c)\overline{Nu}_c/d$ for the hot-gas and cold air flow, respectively, where $\overline{Nu}_h = C(\overline{Pr}_h)^a(\overline{Re}_h)^b$ and $\overline{Nu}_c = C'(\overline{Pr}_c)^{a'}(\overline{Re}_c)^{b'}$ are the average Nusselt numbers. The parameters C, a, b, C', a', b' were calibrated from the energy balance through the HEX, based on CFD calculations.

The effect of the tubes material (typically Inconel) in the overall thermal resistance of the HEX is minor, mainly due to the small thickness of the elliptic tubes walls and the high value of the material thermal conductivity (Yakinthos et al., 2015). Hence, the tubes thermal resistance can be neglected from the calculation of the overall heat transfer coefficient $\overline{U}$, which is computed by $1/\overline{U} = 1/\overline{h}_h + 1/\overline{h}_c$. The HEX effectiveness $\overline{\varepsilon}$ can then be calculated based on the NTU method as a function of

$$\overline{NTU} = \frac{\overline{U}A_s(g,\theta,r,R,N_T)}{\min\{\dot{m}_h\overline{C}_{ph}, \dot{m}_c\overline{C}_{pc}\}} \quad \text{and} \quad \overline{C}_r = \frac{\min\{\dot{m}_h\overline{C}_{ph}, \dot{m}_c\overline{C}_{pc}\}}{\max\{\dot{m}_h\overline{C}_{ph}, \dot{m}_c\overline{C}_{pc}\}}, \tag{4}$$

where $A_s(g,\theta,r,R,N_T)$ is the heat exchange surface, $\overline{C}_{ph}=C_p(\overline{T}_h)$ and $\overline{C}_{pc}=C_p(\overline{T}_c)$.
The aforementioned function, was derived based on previous knowledge and 3D CFD computations of the overall recuperator setup with the use of a porosity model, described in (Yakinthos et al. 2015; Misirlis et al., 2017). It is defined by Eq(5)

$$\overline{\varepsilon}=cf_1\overline{\varepsilon}_1+cf_2\overline{\varepsilon}_2, \tag{5}$$

where $\overline{\varepsilon}_1$ and $\overline{\varepsilon}_2$ are the correlations for one mixed and one unmixed flow streams and both fluids unmixed flow streams, respectively, presented in Kays and London (1984), and cf_1, cf_2 are calibration coefficients. These correlations are defined by Eq(6)

$$\overline{\varepsilon}_1=1/\overline{C}_r\left(1-\exp\left(-\overline{C}_r\left(1-\exp\left(-\overline{NTU}\right)\right)\right)\right),\quad \overline{\varepsilon}_2=1-\exp\left(\overline{NTU}^{0.22}/\overline{C}_r\left(\exp\left(-\overline{C}_r\overline{NTU}^{0.78}\right)-1\right)\right). \tag{6}$$

The heat transfer $\overline{Q}$ of the recuperator can then be calculated by $\overline{Q}=\overline{\varepsilon}\min\{\dot{m}_h\overline{C}_{ph},\dot{m}_c\overline{C}_{pc}\}\left(T_h(1)-T_c(1)\right)$, and the outlet temperatures of the hot-gas and cold air by Eq(7)

$$T_h(2)=T_h(1)-\overline{Q}/\left(\dot{m}_h\overline{C}_{ph}\right)\quad\text{and}\quad T_c(2)=T_c(1)+\overline{Q}/\left(\dot{m}_c\overline{C}_{pc}\right). \tag{7}$$

3. Quantification of the effect of recuperator design on thrust specific fuel consumption

For the rapid quantification of the recuperator effect on the aero engine cycle performance an approach based on the derivation of dedicated trade factors was followed which could time-efficiently reflect the recuperator pressure losses and thermal effectiveness effect on the aero engine Thrust Specific Fuel Consumption (TSFC). These trade factors were derived from analyses of the aero engine thermodynamic cycle performed in GasTurb11 software (Kurzke, 2011). The analyses conditions were corresponding to the IRA engine average cruise conditions, having varying recuperator performance characteristics for the inner and outer pressure losses and the effectiveness (ranging from 0 to 1). The results processing led to the derivation of dedicated trade factors functions (i.e. $h_1(x)$, $h_2(x)$ and $h_3(x)$) for the recuperator pressure loss and heat transfer performance characteristics which described the TSFC percentage change in relation to the reference TSFC (case where no recuperation is applied). Function $h_1(x)$ corresponds to the effect off the recuperator effectiveness on TSCF, $h_2(x)$ corresponds to the recuperator internal pressure losses effect and $h_3(x)$ corresponds to the effect of the external pressure losses on TSFC.
The estimation of the engine TSFC was calculated by Eq(8)

$$h\colon[0,1]^3\to\mathbb{R}\quad\text{defined by}\quad h(x,y,z)=h_1(x)\cdot h_2(y)\cdot h_3(z)\cdot h_r, \tag{8}$$

where h_r is the reference TSFC which is appropriately recalibrated by the derived trade factors function in order to calculate the TSFC of the recuperated aero engine and include all the necessary information regarding the recuperator performance and the aero engine geometrical constraints. For estimating the accuracy of the TSFC values as derived through the use of the trade factors functions, the estimated TSFC values were compared to the ones calculated analytically from GasTurb11. The comparison corresponded to many cases having various recuperator effectiveness and pressure losses values. The results were in close agreement, with the absolute TSFC difference being less than $0.05\ g/(kNs)$, showing that the use of the trade factors functions was of sufficient accuracy for incorporation in the surrogate model for the direct estimation of the IRA engine TSFC.

4. Recuperator design optimization algorithm

In section 2, the recuperator performance characteristics were described, based on a parameterization of the recuperator designs by $p=(g,\theta,r,R,N_T,N_F)$. For fixed p the outlet conditions $x=\left(T_h(2),P_h(2),T_c(2),P_c(2)\right)$ can be computed by solving the system of nonlinear equations $f_p(x)=0$ defined by Eq(2), Eq(3) and Eq(7). Now, given x, an estimation $F(x)$ of the aero engine TSFC (for average cruise conditions), can be obtained from the mapping h defined by Eq(8) using equality Eq(5). In other words, if ε is the mapping $x\mapsto\overline{\varepsilon}$ defined by Eq(5), then $F(x)=h\left(\varepsilon(x),\left(P_c(1)-x(4)\right)/P_c(1),\left(P_h(1)-x(2)\right)/P_h(1)\right)$.
The aero engine geometrical and manufacturing constraints, impose the restriction of the design parameters to the set $S=A\left(\alpha(1),\beta(1),\delta(1)\right)\times\cdots\times A\left(\alpha(6),\beta(6),\delta(6)\right)$ (the design space), where $A(\alpha,\beta,\delta)=\{x\in\mathbb{R}\mid\alpha\le x\le\beta, x=i\delta, i\in\mathbb{N}\},)$. For an arbitrary $p\in S$ the estimation of the engine TSFC corresponding to p, can be computed by the two-step process described in the preceding paragraph: (a) Find a solution y to the system of nonlinear equations $f_p(x)=0$; (b) evaluate F at y. The problem posed is to find the recuperator design (i.e. the point $p\in S$) that minimizes the estimation of the engine TSFC.

The search for the optimal recuperator design (in the sense just described) was performed using the simulated annealing algorithm:

```
1   function simulated-annealing(p_0, r, T_0, T_F, k_T, r-tree)
2       T ← T_0,  p_* ← p ← p_0,  c_* ← c ← eval-tsfc(p_0, r-tree)
3       repeat
4           for i ← 1, k_T do
5               p_n ← neighbor(p)          ▷ Select a point in N(p) = {q ∈ S | |q(i) − p(i)| ≤ δ(i), i = 1,..,6}
6               c_n ← eval-tsfc(p_n, r-tree)
7               if error occured then go to 4
8               if c_n < c then
9                   p ← p_n,  c ← c_n
10                  if c_n < c_* then p_* ← p_n,  c_* ← c_n
11              else
12                  s ← random[0, 1)       ▷ Generate a uniformly distributed number in [0, 1)
13                  if s < exp((c − c_n)/T) then p ← p_n,  c ← c_n
14          T ← rT                         ▷ Geometric cooling schedule (cooling ratio 0 < r < 1)
15      until T < T_F
16      return (c_*, p_*)
17
18  function eval-tsfc(p, r-tree)          ▷ Compute aero engine TSFC corresponding to p
19      (d, (q, z)) ← r-tree.nearest-neighbor(p)
20      if d > 0 then
21          Try to approximate a solution y to the system f_p(x) = 0 using Newton's method with initial
            approximation z; in case of failure, signal an error (and return).
22          r-tree.insert(p, y)            ▷ Store (p, y) in the R-tree data structure
23          return F(y)
24      else return F(z)
```

A detailed exposition of the SA algorithm can be found in Van Laarhoven and Aarts (1987). Regarding its implementation presented in Figure 5, the search for the optimal design starts from a given point $p_0 \in S$ with $T = T_0 < T_F$. The annealing temperature T is updated according to the geometric cooling schedule (line 14), and the sequence of transitions (at constant temperature) from the current point p to a new neighboring point $p_n \in N(p)$ is performed according to the Metropolis criterion (lines 8-13). The output of the algorithm is the point p_* in the subset of S explored during the search that yields the smallest engine TSFC value.

Each invocation of the function eval_tsfc (line 31), requires the solution of a system of nonlinear equations. The strategy for finding good initial approximations to the sought solutions is the following: if $\{p_i\}_1^n \subset S$ are the parameters for which the solutions $\{y_i\}_1^n$ have already been computed (i.e. $f_{p_i}(y_i) \cong 0$) and $f_q(x) = 0$ is the system for which a solution y is sought, then as initial approximation to y, the solution y_j is used corresponding to the nearest neighbor p_j of q in $\{p_i\}$ (with respect to the Euclidean metric d); that is $d(p_j, q) = \min\{d(p_i, q) \mid i = 1, \ldots, n\}$. An alternative strategy is to use the last computed solution as the initial approximation to y. Numerical studies conducted with both strategies, showed that the former can significantly improve the success rate of the algorithm in solving the nonlinear systems, and therefore its ability to avoid local optima.

The implementation of the "nearest neighbor" strategy described in the preceding paragraph was based on the R-tree data structure (Guttman, 1984). R-trees are height-balanced trees with a special structure that allows the implementation of efficient nearest neighbor search algorithms. More information can be found in the references (Manolopoulos et al., 2006). The last argument of the simulated-annealing function is an R-tree data structure, used for indexing the solutions $\{y_i\}$. In the first invocation of the function it contains a single entry (p_0, y), where y is an approximate solution to the system $f_{p_0}(x) = 0$. After each transition from the current point p to a new neighboring point p_n, a nearest neighbor search is performed in the R-tree (line 32). The search returns the entry (q, z), where q is the nearest neighbor of p_n and z is an approximate solution to the system $f_q(x) = 0$, and the distance d from p_n to q. Finally, a solution to the system $f_{p_n}(x) = 0$ is sought (if one has not already been computed, i.e. $d > 0$) using (a variant of) Newton's method (line 34); if the latter converges to a solution y, then the pair (p_n, y) is stored in the R-tree (line 35), otherwise an error is signaled.

In Table 1, the results of a numerical study of the SA algorithm (Figure 5) are shown. In this study, the algorithm was executed for a sequence $(p_i)_0^{500}$ of initial points in S, where the points p_i with $i > 1$ were randomly generated, with $r = 0.9, T_0 = 5.5 \cdot 10^{-3}, T_F = 10^{-8}$ and $k_T = 600$.

Table 1: Numerical study results.

	Parameters variation % for Optimal recuperator design in relation to Initial recuperator design (p_0)
$(g, \theta, r, R, N_T, N_F)$	$(0, -24.986, 0, +6.667, +27.273, -50)$
$\overline{\varepsilon}$	$+7.259$
Engine TSFC	-2.246

5. Conclusions

At the present work the development of a process for the optimization of the geometrical characteristics of a recuperator developed for aero engine applications was presented. This process was taking into account the main aero engine geometrical constraints and limitations, so as to lead to feasible recuperator designs. The methodology was based on dedicated numerical surrogate tools which directly linked the effects of the most important geometrical recuperator features on the recuperator operational performance characteristics. In this work, a nonlinear surrogate model based on the use of the simulated annealing algorithm, which incorporated the major geometrical features of the recuperator and included high-fidelity pressure losses and heat transfer correlations was developed. With the use of this model the recuperator performance was optimized by achieving a ~2.25 % TSFC reduction showing the usefulness of this model in design optimization studies.

Acknowledgments

The studies were conducted in the project ULTIMATE ("Ultra Low emission Technology Innovations for Mid-century Aircraft Turbine Engines"). This project received funding from the European Union's Horizon 2020 research and innovation programme under grant agreement No 633436. Christina Salpingidou would like to thank Alexander S. Onassis Public Benefit Foundation for the scholarship.

References

ACARE: Advisory council for aviation research and innovation in europe, 2012, Strategic Research & Innovation Agenda <http://www.acare4europe.org/sites/acare4europe.org/files/ attachment/acare-strategic-research-innovation-volume-1-v2.7-interactive-fin_0.pdf> accessed 18.04.2018.

Anderson, J.D., 2011, Fundamentals of aerodynamics, 5th ed., McGraw-Hill: New York, NY, USA.

Guttman, A., 1984, R-trees: A dynamic index structure for spatial searching, SIGMOD Rec. 14, 47–57.

Kays W., and London A., 1984, Compact heat exchangers, mcgraw-hill company, Inc., New York, USA.

Kurzke J., 2011, Design and off-design performance of gas turbines, GasTurb11 user's manual, GasTurb GmbH, Germany.

LEMCOTEC: Low Emissions Core-Engine Technologies Project, <www.lemcotec.eu> accessed 19.04.2018.

Manolopoulos, Y., Nanopoulos, A., Papadopoulos, A.N., Theodoridis, Y., 2006, R-Trees: theory and applications. Springer London, London, UK.

Misirlis D., Vlahostergios Z., Flouros M., Salpingidou C., Donnerhack S., Goulas A., Yakinthos K., 2017, Optimization of heat exchangers for intercooled recuperated aero engines, Aerospace, 4(1), 14.

NEWAC, 2018, New aero engine core concepts project, <www.newac.eu> accessed 18.04.2018.

Pratt, R.M., 2001, Thermodynamic properties involving derivatives: using the Peng-Robinson Equation of State, Chemical Engineering Education, 35(2), 112-139.

Salpingidou C., Misirlis D., Vlahostergios Z., Flouros M., Donnerhack S., Yakinthos K., 2016, Numerical modeling of heat exchangers in gas turbines using CFD computations and thermodynamic cycle analysis tools, Chemical Engineering Transactions, 52, 517-522.

Van Laarhoven, P.J., Aarts, E.H., 1987, Simulated annealing annealing: Theory and applications. Springer, Dordrecht, The Netherlands.

Yakinthos K., Misirlis D., Vlahostergios Z., Flouros M., Donnerhack S., Goulas A., 2015, Best strategies for the development of a holistic porosity model of a heat exchanger for aero engine applications, Proceedings of ASME Turbo Expo 2015: Power for Land, Sea and Air, ASME, Montreal, Canada.